

Numerical Study on Cooling Characteristics in Channels with Pin Fin Arrays under High Temperature/Pressure Conditions

S.-E. Peng, W. JIN, J.-M. WU *

State Key Laboratory for Strength and Vibration of mechanical Structures
Shaanxi Key Laboratory of Environment and Control for Flight Vehicle
School of Aerospace, Xi'an Jiaotong University
Xi'an, Shaanxi, 710049, China
*Email: wjmxjtu@mail.xjtu.edu.cn

Abstract

Channel with pin fin arrays is often used in the internal cooling of the trailing edge of the turbine blade. Most researches on the internal cooling characteristics are carried out experimentally or numerically at conditions of atmospheric air inlet and low heat load (defined as the ratio of isothermal wall temperature to the cooling air inlet temperature) on the channel wall. However, the cooling conditions for the actual turbine blade are at high air inlet temperature/pressure and high heat load. To understand the effects of the air inlet and heat load conditions on the cooling performance of channels with pin fin arrays, a CFD numerical simulation study was carried out through FLUENT. The numerical results show that with the increase of heat load on the channel wall, the heat transfer performance in the channel decreases and the friction factor in the channel increases. In comparison with the atmospheric air inlet conditions, high air inlet temperature/pressure conditions cause the decrease in the heat transfer capacity of the channel, and the decrease is more significant at high heat load conditions. While the air inlet condition has little influence on friction factor of the channel. With the increase of air inlet Reynolds number (Re), the Nusselt number (Nu) number in the cooling channel at high air inlet temperature/pressure and high heat load conditions decreases more in comparison with that at atmospheric air inlet temperature/pressure and low heat load conditions. This decrease should be considered in the design the internal cooling structure of actual turbine blades.

Keywords: Pin fin arrays channel; Flow and heat transfer; Thermal boundary condition, Inlet flow condition

1. Introduction

Aero gas turbine engines with high thrust-weight ratios put forward higher requirement for the cooling design of the high temperature components. The studies on the internal and film cooling of the turbine blade have been a hot issue for scientists and engineers till now. Pin fin arrays are often used in the internal cooling of the trailing edge of the turbine blade [1], because that pin fin arrays not only disturb the flow field for heat transfer enhancement but also provide the components with additional structural support. Some previous investigations on the characteristics of the internal cooling channel with pin fin arrays are reviewed in the followings. Metzger et al. [2] analyzed the influence of different spacing of pin fin arrays on heat transfer performance in rectangular channels. They observed that the reduction of the streamwise spacing of the pin fin arrays can effectively improve the heat transfer effect in the passage. Chyu et al. [3] studied the influence of the arrangement of pin fins on the Nusselt number in the channel. Their results showed that although the staggered array increased flow loss, it effectively improved the heat transfer effect in the channel. According to Chyu et al. [4], long pin fin arrays with high aspect ratio provide more areas with good heat transfer on the surface of the pin fins. So, the heat transfer enhancement effect of long pin fins is better than short pin fins. Considering the flow loss and heat transfer effect comprehensively, the pin fin arrays with an aspect ratio of 2 are considered to have better effect. Some researchers also studied the influence of the shape of pin fins and the channel size on the flow and heat transfer in the cooling channel. Jin et al. [5] investigated 6 pin fin structures with cross section of circular, elliptic, teardrop, lancet and NACA,

respectively. It is observed that the NACA pin fin arrays with optimized streamwise/spanwise spacings had better comprehensive cooling performance. Siw et al. [6] studied the effect of pin fin arrays on the flow and heat transfer in the narrow channel. They pointed that the narrow channel had better enhancement effect than the wide channel under the same distribution density of pin fin arrays.

Now it is known that pin fin arrays significantly improve the heat transfer effect in the channel. For deeper analysis, some researchers tried to make clear the contribution of pin fin arrays to the heat transfer enhancement on the endwall and pin fins' surface [7, 8]. Chyu et al. [8] found the cooling effect of the endwall behind the pin fins was improved, while the difference of the heat transfer coefficient was only 10% to 20% between the endwall and pin fins' surface. Based on this finding, in a large number of experimental studies on the heat transfer in the channel with pin fin arrays, only the endwall heat transfer was measured [9-11].

So far, there are a lot of experimental studies on the flow and heat transfer characteristics in the channel with pin fin arrays. However, with the limitation of experimental techniques and cost, the experimental studies using the naphthalene sublimation technique or the transient liquid crystal technique are carried out under the atmospheric air inlet and small heat transfer temperature difference between the wall temperature and air inlet temperature ($T_w - T_{in}$). However, under engine actual operating conditions, the turbine blade surface temperature is about 1200K, and the cooling air flow in the internal cooling channel is from the compressor, which has high pressure and a temperature above 600K. Such conditions result in a large ratio of blade wall temperature to inlet cooling air temperature, which is defined as heat load in this paper. Under the conditions of high air inlet temperature/pressure and high heat load, the flow and heat transfer performance in the channel with pin fin arrays should be different from that obtained under atmospheric air inlet and low heat load conditions. Understanding this difference is very important to reasonably modify the experimental results to make reliable cooling design of actual turbine blades. However, research on this issue is not much till now.

Lee et al. [12] studied the influence of high-temperature inlet airflow on the flow field and heat transfer in the pin fin arrays channels under high heat load. The results show that the flow in the channel is more stable and vortex shedding occurs later under high heat load. This indicates that the high heat load conditions change the flow field structure inside the channel, and the heat transfer characteristics are also different from that obtained under the atmospheric inlet temperature conditions. It should be noted that even in Lee et al.'s study [12], high pressure condition of air inlet is not taken into consideration. Therefore, the present study is to check the influence of air inlet and heat load conditions on internal cooling performance of channel with pin fin arrays using numerical simulation method.

2. Problem statement and numerical method

2.1 Physical model

Chyu et al. [4] carried out a series of experimental studies under low heat load conditions and atmospheric air inlet conditions by using naphthalene sublimation technique on the pin fin arrays channel. Their experimental results are cited by many researchers as classic literature. In this paper, the computational geometry model to be simulated is based on the experimental section of Chyu et al. [4], as shown in Figure 1.

The computational model is a rectangular channel with short pin fin arrays ($H/D=1$). There are 7 rows of short pin fin arrays on the wall of the channel. The diameter of the pin fin is $D=0.0127\text{m}$. The spanwise spacing is S and the streamwise spacing is X , with $X=S=2.5D$. The rectangular channel is $L=0.864\text{m}$ and divided into three parts along the flow direction (x direction): the front extension section ($19D_h$), the test section of $L_e=0.1825\text{m}$ (arranging staggered pin fin arrays) and the back extension section ($10D_h$). The width (y direction) of the computational model is $W=0.0795\text{m}$, which is only half of the experimental model [4] due to the symmetry in y direction.

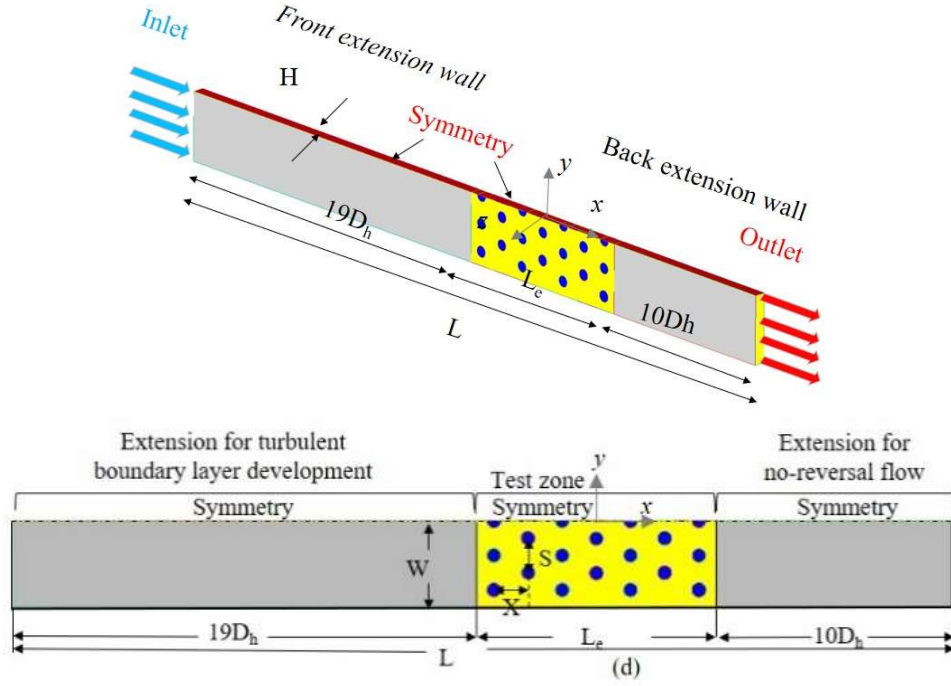
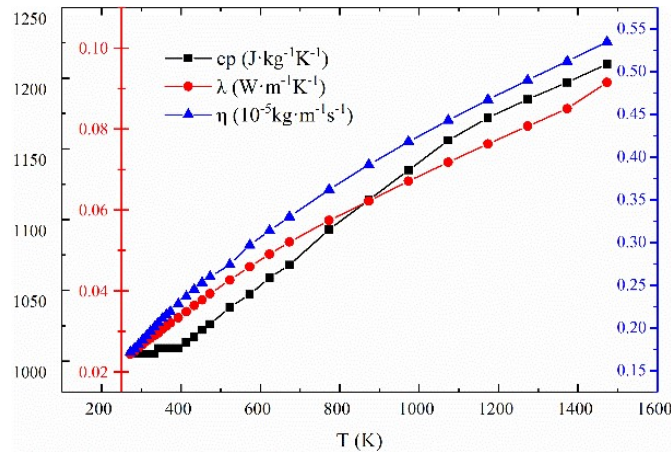


Figure 1 - Computational geometry model.

2.2 Numerical models and methods

As mentioned above, the inlet air of the internal cooling channel of the actual turbine blade is the discharged air from compressor and under high temperature/pressure conditions. The heat load of the channel is also under high level. That means the thermo-physical properties of the air inside the cooling channel are different from those under atmospheric air inlet and low heat load conditions. Thus, the present paper considers the change of air thermos-physical properties with temperature and pressure. Ideal gas state equation is used to consider the change of air density with temperature and pressure. As we know, the specific heat capacity of c_p , the thermal conductivity of λ and the dynamic viscosity of η of air are almost independent of pressure, the change of these three thermos-physical properties with temperature as shown in Figure 2, are fitted in polynomials, and written in UDF files in the definition of the thermo-physical properties of air.


 Figure 1 - Change curve of c_p , λ , η of air with temperature

Continuity, momentum and energy equations with consideration of the change of the thermos-physical properties of air are used to solve the air flow and heat transfer in the channel. It should be noted the coupled heat conduction inside the pin fins with air flow is considered by solving the heat conduction equation at the same time. All the governing equations are not written here for brevity.

The channel is set as mass flow rate inlet and pressure outlet boundary. The wall of heating section on which pin fin arrays are equipped is assigned with isothermal wall temperature which refers to the

heat load value. The symmetry walls of whole channel and pin fins ($y=0$) are set as the symmetry boundary. The other walls include that of front/back extension zone and heating section are adiabatic with non-slip boundary.

Two air inlet conditions are defined in this paper: atmospheric inlet condition (*atmo.*) where the air inlet the pressure is 1atm, temperature is 287K; High air inlet pressure/temperature condition (*act.*) to simulate the actual air inlet condition of cooling channel, where the air pressure is 1.051×10^6 Pa and the temperature is 633K. The inlet Reynolds number is from 5000 to 100000, the heat load (T_w/T_{in}) is from 1.1 to 1.9 for the two air inlet conditions. Under the *act.* air inlet condition, the air inlet temperature is 633K, the case with heat load of 1.9 can simulate closely the actual working condition of the internal cooling passage in turbine blade with the blade wall temperature up to 1200K.

2.3 Data reduction

The Reynolds number (Re) of the inlet air flow is defined as Eq. (1). Under the given inlet mass flow rate (q_m), the dynamic viscosity coefficient is taken as the value at air inlet temperature T_{in} , the characteristic velocity is the inlet air average velocity.

$$Re = \frac{\rho_{in} u_{in} D_h}{\eta(T_{in})} = \frac{q_m D_h}{\eta(T_{in}) A_{in}} \quad (1)$$

Where the hydraulic diameter of the channel $D_h = 0.0235$ m; q_m is the mass flow rate in the channel, kg/s; A_{in} is the inlet cross section area ($=H \times W$), m^2 ; u_{in} is the inlet air average velocity, m/s, varying with the inlet mass flow rate and density.

The average heat transfer effect of the cooling air on the endwall is expressed by the average convective heat transfer coefficient which is defined as Eq. (2):

$$q = \frac{c_p (T_{av}) q_m \Delta T}{A_b} \quad (2)$$

$$h = \frac{q}{T_w - T_{av}} \quad (3)$$

Where q is the equivalent heat flux of the channel end wall, W/m^2 ; T_{av} is the characteristic temperature, taking the average temperature of the fluid from inlet to outlet of the heating section, K; ΔT is the average static temperature difference between the outlet and the inlet of the heating section, K; A_b is the total area of the heated endwall ($=2 \times L_e \times W$), m^2 . T_w is the endwall temperature based on the inlet air temperature and the heat load, K.

The average Nusselt number in the channel Nu is defined as Eq. (4).

$$Nu = \frac{h D_h}{\lambda(T_{av})} \quad (4)$$

It is worth mentioning that some literatures averaged the heat flux to the total wall surface of area A , including the end wall surface of the channel and the pin fins surface, as shown in Eq. (5). This is also used in the data reduction of Chyu et al. [4]. Since A is much larger than A_b and q_e is much smaller than q , the average convective heat transfer coefficient of h_e and the average Nusselt number of Nu_e calculated according to Eq. (2) and Eq. (3) are even smaller than the Nu_0 of the smooth channel without pin fin arrays. The heat transfer enhancement by using pin fin arrays is hard to describe by comparing Nu_e with Nu_0 . Therefore, in this paper, we believe that it is reasonable to use Eqs. (1-4) to calculate the average heat transfer of the channel.

$$q_e = \frac{c_p (T_{av}) q_m \Delta T}{A} \quad (5)$$

The friction factor of the channel is defined as

$$f = \frac{\Delta p D_h}{L_e \rho_{in} u_{in}^2 / 2} \quad (6)$$

Where Δp is pressure drop across the heating section, Pa.

2.4 Grid independence assessment

In this paper, fluid-solid coupling heat transfer calculation is carried out. Fluid and solid regions of pin fins are divided into structured grids by ICEM CFD. Figure 3 shows the generated grids, and boundary layer grids are drawn on the sides of the pin fins and the upper and lower end walls of the channel. Four grid systems are generated for the grid independence assessment, which are 1.78, 2.4, 3.08 and 4.1 million, respectively. Figure 4 shows the comparison of the Nu_e in a channel with an inlet Re of 15000 and Realizable k- ϵ turbulence model in the simulation. It can be seen that Nu_e hardly changed with grid number of 3.08 to 4.10 million. Therefore, the grid number of 3.08 million is suitable to obtain grid independent solution and is adopted in the subsequent calculations.

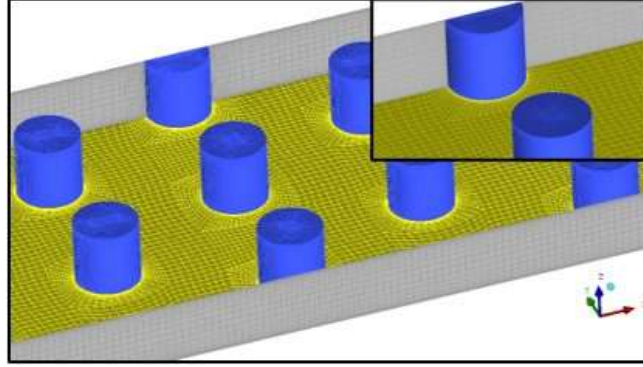


Figure 3 - Grid division

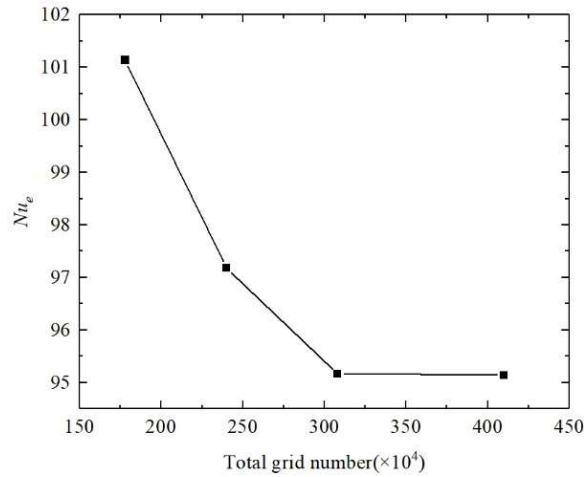
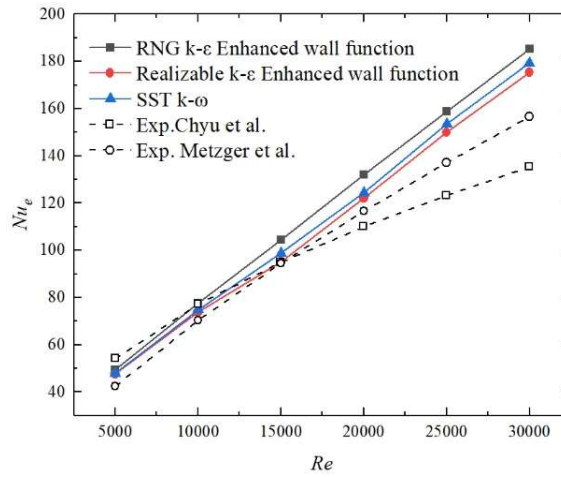


Figure 4 - Variation of Nu_e with total grid number

2.5 Turbulence model verification

In order to predict the flow and heat transfer accurately, the applicability of three turbulence models is checked in this study. They are RNG k- ϵ (Enhanced wall function), Realizable k- ϵ (Enhanced wall function) and SST k- ω . Figure 5 shows the Nu_e calculated by using the three turbulence models in the channel under the experimental conditions. The numerical results are compared with the experimental results from Chyu et al. [4] and Metzger et al. [3]. It is worth mentioning that, Chyu et al. [4] discussed their experimental results and considered that their results were more accurate under low Re condition, while Metzger et al. [3] were more accurate under high Re condition.

It can be seen that the results using Realizable k- ϵ model with enhanced wall function are more consistent with the experimental results. The maximum error under low Re condition (≤ 20000) was 7.40% in comparison with the experimental results of Chyu et al. [4]. While the maximum deviation was 12.04% under high Re condition in comparison with the results of Metzger et al. [3]. Therefore, the Realizable k- ϵ turbulence model is used in the following calculations.


 Figure 5 - Comparison of Nu_e with different turbulence models

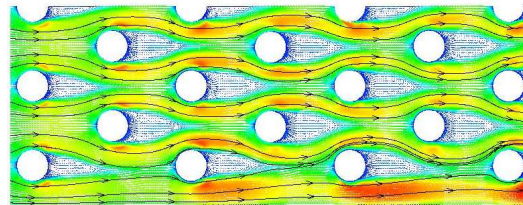
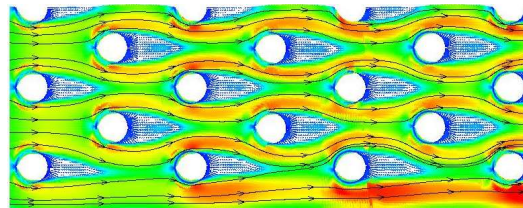
3. Result and discussion

3.1 Effect of heat load under the same air inlet condition

Velocity distribution

The channel with pin fin arrays at inlet $Re=60000$ under *act.* air inlet conditions are chosen as an example in this part. In order to better understand the characteristics of heat transfer and friction in the channel, the flow fields in the channel are analyzed.

Figure 6 shows the distribution of the velocity V_{xy} on the center plane in the Z direction ($z=0$) under three heat load conditions. The typical characteristics of fluid flow in the channel with pin fin arrays are similar for the three cases. As the air flows through the channel with staggered pin fin arrays, V_{xy} increases continuously from the inlet to the outlet of the channel. The reason is that air absorbs heat along the way, the temperature increases and the pressure decreases. This is particularly significant under high heat load conditions, which leads to the acceleration of gas because of the expansion of air. The leading edges of each row of pin fins are impacted differently by the incoming flow. The incoming flow impacts the first row of pin fins with greater strength, because of the obstruction of the first row of pin fins to the flow area of the channel, the velocity of the airflow before the second is increased and the impact strength to the second row of pin fins increases. However, after the airflow passes through the first and second rows of pin fins, the airflow is mixed and the flow direction is deflected, and the impact effect on the leading edge of the rear pin fins is weakened. As shown in Figure 6, when the airflow flows through the pin fin arrays, flow separation occurs behind the pin fins, and finally forming a wake area at the trailing edge.


 (a) $T_w/T_{in}=1.1$

 (b) $T_w/T_{in}=1.5$

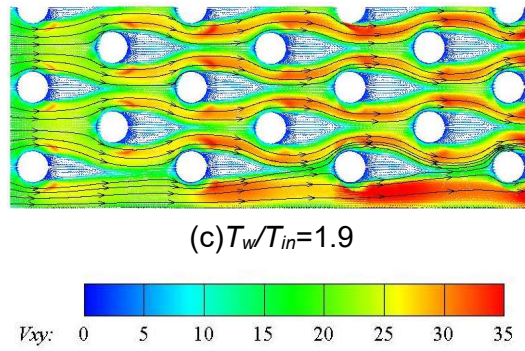


Figure 6 - V_{xy} distribution on the central plane in z direction ($z=0$) under different heat loads

Nusselt number distribution

Figure 7 shows the distribution of local Nu number on the end wall of the heating section of the rectangular channel under three heat load conditions. It can be seen that the local Nu number at the leading edge of the pin fin is high due to the impact of incoming flow. The local Nu number at the second row's leading edge is the largest with a the "U-shaped" zone. After that, the heat transfer at the leading edge of the pin fins gradually decreases with the number of rows. As shown in Figure 6, the velocity of inlet flow increases after flowing through the first row of pin fins of rectangular channel. Therefore, the impact velocity on the leading edge of the second row of pin fins is large and the heat transfer is enhanced. After the airflow passes through the first and second rows of pin fins, the airflow is mixed and the flow direction is deflected, and the impact effect on the front edge of the rear pin fin arrays is weakened, leading to a decrease in the local heat transfer of the rear pin fin arrays.

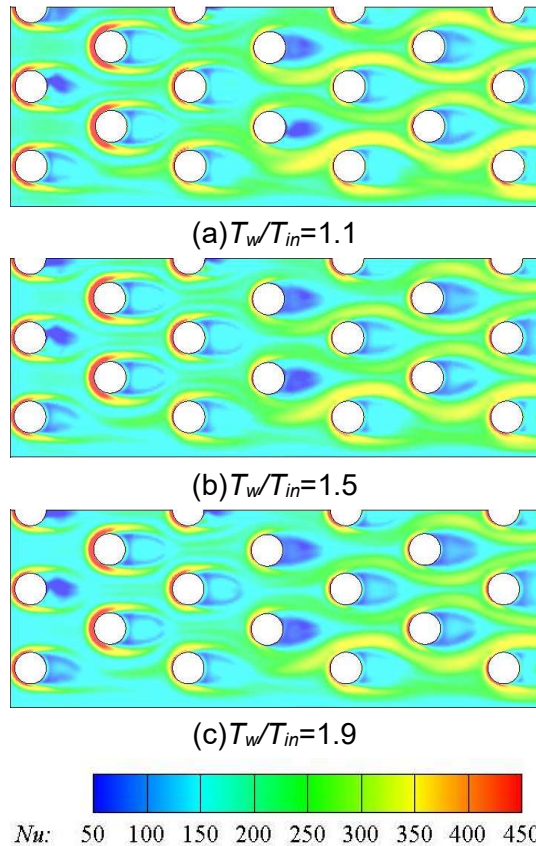


Figure 7 - Nu number distributions under different heat loads

The heat transfer in the regions between the spanwise neighboring pin fins gradually increases with the number of rows. It is also related to the velocity field distribution characteristics as mentioned above. When the air is being heated along the flow direction, the airflow between the spanwise neighboring pin fins expands and accelerates. The heat transfer between the airflow and the wall surface is enhanced. At the same time, the physical properties of the air change with the increase of

temperature, which has a negative impact on the heat transfer of the fluid-wall interface. However, the acceleration of the air flow has a larger impact on heat transfer between the spanwise neighboring pin fins, and overall the heat transfer is enhanced.

Figure 7 shows the wake area of fourth row pin fin has the worst heat exchange, while in the trail region behind each pin fin the heat transfer performance improves with the increase of row number. This is because the velocity of secondary flow along the flow direction decreases in the wake area, which weakens the heat transfer. However, in the latter rows, the accelerated expansion of the main airflow carries more heat away, which results in a combined effect of enhanced heat transfer in the wake area of the rear pin fins.

Variation of Row-average Nu and friction factor

Figure 8 shows the variation of average Nu around each row of pin fins on the end wall with the number of rows under three kinds of heat loads. By comparing the distribution of Nu number under $T_w/T_{in}=1.1$ and 1.9 in Figure 7 and Figure 8, it can be found that high heat load reduces the heat transfer performance of each part in the channel, especially in the leading edge and the wake area. For the zone around the 1st and 2nd rows of pin fins, due to the short heating time, the air physical properties change little and the local Nu number slightly decreases with the heat load. After the 3rd row of pin fins, with the increase of the heating time, the change of physical properties and the acceleration of the air flow reduce the heat transfer on the channel under high heat load conditions. The variation of Nu number and friction factor with heat load T_w/T_{in} are shown in Figure 9. The Nu number under $T_w/T_{in}=1.9$ decreases by 13.32% in comparison with that under $T_w/T_{in}=1.1$. The friction factor f of rectangular channel increases with the increase of heat load. There are two reasons for the increase of friction factor the in the channel with increased heat load. First, with the increase of the heat load, the air viscosity increases (see Figure 2). Second, under high heat load, the expansion of air along the streamwise direction becomes more significant, which leads to the increase of pressure drop.

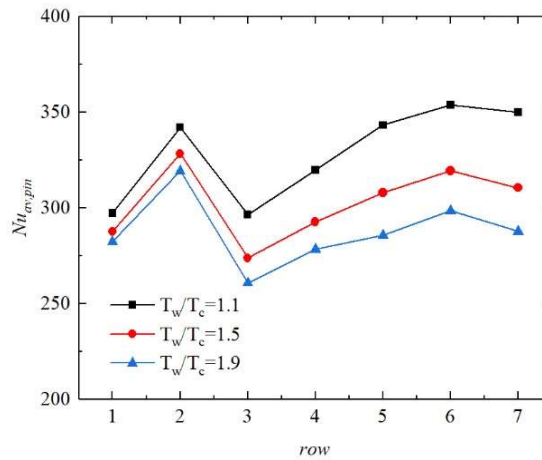


Figure 8 - Variation of Nu number around each pin-fins' row under different heat loads (Re=60000)

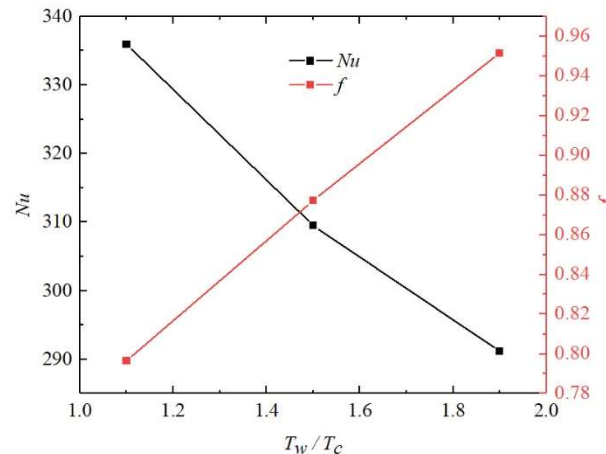


Figure 9 - Variation of Nu and f with heat load (Re=60000)

3.2 Effect of heat load under different air inlet conditions

The air inlet conditions and the heat load mainly affect the temperature and pressure of the air in the cooling channel, which lead to the change of physical properties of cooling air.

Figure 10 shows the variation of Nu number of both end walls and channel friction factor f with heat load under two air inlet conditions. It is found that the air inlet condition has little effect on the channel friction factor f under the same heat load conditions. Under the same inlet Re number condition, the inlet temperature is high and the aerodynamic viscosity coefficient is large. According to Eq. (1), the mass flow rate of airflow also increases. But the pressure drop of the channel still increases under the *act.* air inlet condition due to the increase of air dynamic viscosity and the acceleration of airflow in comparison with that under *atmo.* air inlet condition.

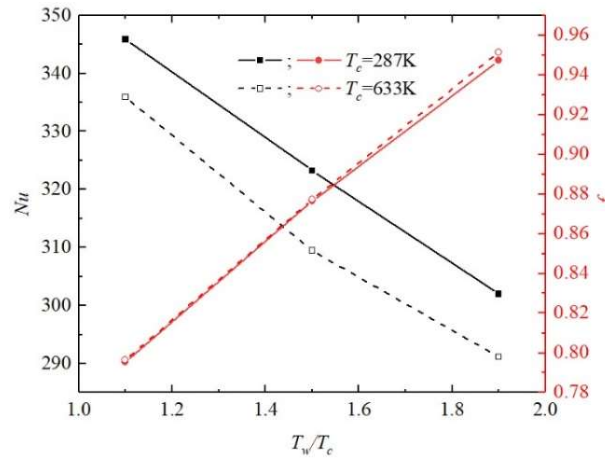


Figure 20 - Variation of Nu and f with heat loads (Re=60000)

Figure 10 also shows that under the same heat load condition, the average Nu number on the end wall under the *act.* air inlet condition is significantly smaller in comparison with that under the *atmo.* air inlet condition. As mentioned above, most of the current experimental research results are based on *atmo.* air inlet conditions and low heat load conditions, but the actual working conditions of turbine blades are *act.* air inlet conditions and high heat load conditions. The calculated results in this paper show that the average Nu number of the endwall under the *act.* air inlet condition and high heat load decreases by 15.8% in comparison with that under the *atmo.* air inlet condition and low heat load.

3.3 Effect of Reynolds number under different air inlet conditions

As shown in Figure 11 and Figure 12, the Nu number increases with the Re number under the two different conditions. The condition 1 is experimental condition which is defined as *atmo.* air inlet condition and heat load=1.1. The condition 2 is actual condition which is defined as *act.* air inlet condition and heat load=1.9. In the low range of Reynolds, the difference of Nu between condition 1 and condition 2 is small. Such difference between the two conditions increases with the increase of Re number. Under the condition of Re=100000, the Nu of cooling channel under condition 2 decreases about 18.37% in comparison with that under condition 1.

The process of turbine cooling structure design includes the selection of cooling structure efficiency parameters. In this step, if the designer set the cooling efficiency of the cooling structure with reference to the experimental value, then the total cooling efficiency obtained in actual working conditions may not meet the requirements. In the meantime, if a conservative modification is set, there will be redundant designs in the turbine blades, which leads more cost and higher weight of turbine engine. Therefore, the results of this paper also indicate that the experimental cooling characteristics need to be carefully calibrated before being used for the turbine cooling design.

Numerical study on Pin-fin arrays Channel under Different Conditions

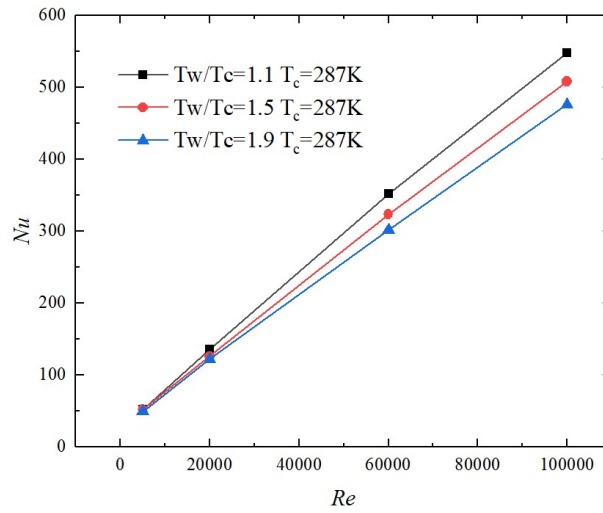


Figure 31 - Effect of Re under *atmo.* air inlet condition

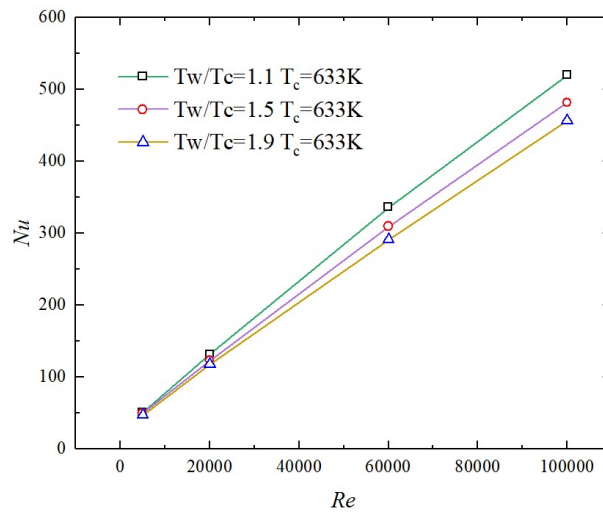


Figure 42 - Effect Re under *act.* air inlet condition

4. Conclusion

In this paper, the influence of endwall heat load and cooling air inlet conditions on the heat transfer characteristics of the flow in the channel with pin fin arrays is studied by numerical simulation. The main conclusions are as follows:

- (1) Under the same inlet flow condition, the increase of heat load of the endwall leads to the decrease of the average Nu number and the increase of the friction factor in the internal cooling channel with pin fin arrays.
- (2) Under the same heat load and inlet Re number, the average Nu number of the channel under *act.* air inlet condition decreases in comparison with that under *atmo.* air inlet condition. While air inlet condition has little influence on the friction factor of the channel, the pressure drop of the channel still increases under the *act.* air inlet condition due to the increase of air dynamic viscosity and the acceleration of airflow.
- (3) The average Nu number under *act.* air inlet condition and high heat load is lower than that under *atmo.* air inlet condition and low heat load. With the increase of Reynolds number, the difference between them increases. When $Re=60000$, the difference between them is 15.8%. Based on this reason, the experimental results obtained from the atmospheric air inlet and low heat load conditions need to be carefully calibrated before being applied to the design of the actual turbine blade internal cooling structure.

Copyright Statement

The authors confirm that they, and/or their company or organization, hold copyright on all of the

original material included in this paper. The authors also confirm that they have obtained permission, from the copyright holder of any third-party material included in this paper, to publish it as part of their paper. The authors confirm that they give permission, or have obtained permission from the copyright holder of this paper, for the publication and distribution of this paper as part of the ICAS proceedings or as individual off-prints from the proceedings.

References

- [1] Han J-C. Turbine blade cooling studies at texas a&m university: 1980-2004[J]. *Journal of Thermophysics and Heat Transfer*, 2006, 20(2): 161-187.
- [2] Metzger D E, Berry B A, Bronson J P. Developing heat transfer in rectangular ducts with staggered arrays of short pin fins[J]. *Journal of Heat Transfer*, 1982.
- [3] Chyu M K. Heat transfer and pressure drop for short pin-fin arrays with pinendwall fillet[J]. *Journal of Heat Transfer*, 1990, 112: 926-932.
- [4] Chyu M K, Siw S C, Moon H K. Effects of height-to-diameter ratio of pin element on heat transfer from staggered pin-fin arrays[C]. *Proceedings of ASME Turbo Expo*, 2009.
- [5] Jin W, Jia N, Wu J, et al. Numerical study on flow and heat transfer characteristics of pin-fins with different shapes[C]. *Turbomachinery Technical Conference and Exposition*, 2019.
- [6] Siw S C, Fradeneck A D, Chyu M K, et al. The effects of different pin-fin arrays on heat transfer and pressure loss in a narrow channel[C]. *Turbine Technical Conference and Exposition*, 2015.
- [7] Lau S C, Kim Y S, Han J C. Local endwall heat/mass-transfer distributions in pin fin channels[J]. *Journal of Thermophysics and Heat Transfer*, 1987, 1(4): 365-372.
- [8] Chyu M K, Hsing Y C, Shih T I-P, et al. Heat transfer contributions of pins and endwall in pin-fin arrays effect of thermal boundary condition modeling[J]. *Journal of Turbomachinery*, 1999, 121.
- [9] Axtmann M, Poser R, Von Wolfersdorf J, et al. Endwall heat transfer and pressure loss measurements in staggered arrays of adiabatic pin fins[J]. *Applied Thermal Engineering*, 2016, 103: 1048-1056.
- [10] Zhu H, Guo T, Zhang L et al. Measurement of endwall heat transfer in pin-fin array duct with lateral-flow by using transient liquid crystal technique[J]. *Journal of Propulsion Technology*, 2007, 28: 620-623.)
- [11] Jenkins S C, Shevchuk I V, Wolfersdorf J V, et al. Transient thermal field measurements in a high aspect ratio channel related to transient thermochromic liquid crystal experiments[J]. *Journal of turbomachinery*, 2012.
- [12] Lee C-S, Shih T I-P, Bryden K M, et al. Effects of high heating loads on unsteady flow and heat transfer in a cooling passage with a staggered array of pin fins[C]. *Turbomachinery Technical Conference and Exposition*, 2019.